Practical Sub-Nyquist Sampling via Array-based Compressed Sensing Receiver Architecture

Andrew K. Bolstad*, James Edwin Vian*, Jonathan D. Chisum†, and Youngho Suh*
*MIT Lincoln Laboratory
Lexington, MA 02420–9108
Email: {andrew.bolstad, vian, youngho.suh}@ll.mit.edu
†Department of Electrical Engineering
University of Notre Dame
South Bend, IN 46556
Email: jchisum@nd.edu

***Abstract*—This paper introduces the Array-based Compressed sensing Receiver Architecture (ACRA). ACRA allows digital receiver arrays to operate at dramatically larger instantaneous bandwidths by sampling the signals from different array elements at different sub-Nyquist sampling rates. Signal processing inspired by the sparse fast Fourier transform allows for signal detection, estimation, and angle-of-arrival determination. Simulation results and measurements from an 18–45 GHz testbed are presented.**

I. Introduction

Fully digital phased array receivers typically operate over instantaneous bandwidths which are much less than their tuning bandwidths due to limitations in ADC sampling rates or data processing capability. The local oscillator frequency must be set using either a cueing receiver or prior knowledge of the band of interest. While tuned to a particular frequency band, such an array cannot demodulate, decode, or determine the angle-of-arrival (AoA) of signals in different bands.

In theory Compressed Sensing (CS) can extend instantaneous bandwidth beyond Nyquist rate limitations [1], [2]; however, receivers using CS techniques typically require significant changes to front-end RF hardware [3], [4], [5], [6]. Furthermore, CS signal reconstruction algorithms can be computationally demanding (REF). The related sparse Fourier transform algorithms aim to reduce the processing time necessary to compute the DFT of frequency-sparse signals [7]. In particular, the sparse fast Fourier transform (sFFT) achieves processing time better than the ubiquitous FFTW for long, frequency-sparse signals using only a small subset of the available data [8].

The sFFT operates on a length-N signal by subsampling (modulo N) by L different integer factors producing L data streams. A window function applied to each data stream significantly reduces the number of samples actually used. This compressed set of measurements contains L versions of the original signal, each experiencing a different pattern of aliasing. The sFFT resolves the ambiguity present in any single data stream by combining all L versions of the aliased signal in a voting procedure (see Sec. II for a detailed description of the sFFT).

The subsampling step of the sFFT can take place in the analog-to-digital conversion step of an RF receiver by using L different ADCs, each operating at a different sub-Nyquist sampling rate. Along these lines, the "BigBand" receiver replaces a single high cost, power hungry Nyquist rate ADC with several low rate, low power ADCs to sample the signal from a single antenna [9]. Taking advantage of the N_r ADCs already available in a fully digital receiver array with N_r antenna elements, we propose operating these ADCs at $L \leq N_r$ different sampling rates. The digital data aquired from each element can then be processed as prescribed by the sFFT to recover the frequency support of sparse spectral signals. Furthermore, the sFFT can be modified to leverage the spatial diversity of the array, providing AoA capability as well as a coherent estimate of the signal.

This paper describes our Array-based CS Receiver Architecture (ACRA). The remainder of the paper is organized as follows. Section II describes the sparse fast Fourier Transform developed in [8]. Next, Sec. III describes how sFFT signal processing can be used to drastically increase the input bandwidth of a receiver array. A few simulations illustrate the concept in Sec. IV, and Sec. V gives a few initial results from our 18–45 GHz ACRA testbed. A summary is given in Sec. VI.

II. Sparse Fast Fourier Transform Review

ACRA was inspired by the sFFT described in [8], which we summarize here. The sFFT makes use of a "hash function" $h_\sigma : [N] \to [B]$ and "offset" $o_\sigma : [N] \to [\frac{-N}{2B}, \frac{N}{2B}]$ given by:

$$h_\sigma(i) = \left\lfloor \frac{\sigma i B}{N} \right\rceil$$

$$o_\sigma(i) = \sigma i - h_\sigma(i)\frac{N}{B}$$

Distribution A: public release, unlimited distribution. This work is sponsored by the Assistant Secretary of Defense for Research & Engineering under Air Force Contract #FA8721-05-C-0002. Opinions, interpretations, conclusions, and recommendations are those of the authors and are not necessarily endorsed by the United States Government.

The notation $[N]$ denotes the set $\{0, 1, \ldots, N-1\}$, and $\lfloor x \rceil$ means round x to the nearest integer. Each "inner loop" of the sFFT uses a downsampling factor σ and delay τ. These are selected uniformly at random from $[N]$ with the restriction that σ is relatively prime to N. The sFFT comprises the following steps:

Location Inner Loop For $l \in \{1, 2, \ldots, L\}$, run a location inner loop to get I_l.

1) Downsample and window the data: $y_i = w_i x_{\sigma i + \tau}$.
2) Compute $Z_k = Y_{k(N/B)}$ for $k \in [B]$. This is the DFT of $z_i = \sum_{j=0}^{\lceil w/B \rceil - 1} y_{i+jB}$.
3) Let J contain the dk coordinates of maximum magnitude in Z. Return $I_l = \{i \in [N] : h_{\sigma_l}(i) \in J\}$.

Vote For each $i \in I = \bigcup_{l=1}^{L} I_l$, let $s_i = |\{l : i \in I_l\}|$.

Threshold Let $\hat{I} = \{i \in I : s_i \geq T_d\}$

Estimation Inner Loop For $l \in \{1, 2, \ldots, L\}$, run an estimation inner loop on $\hat{I}$ to get $\hat{X}^{(l)}$.

1) Downsample and window the data: $y_i = w_i x_{\sigma i + \tau}$.
2) Compute Z_k, the DFT of $z_i = \sum_{j=0}^{\lceil w/B \rceil - 1} y_{i+jB}$.
3) For $i \in \hat{I}$, estimate X_i as $\hat{X}_i^{(l)} = Z_{h_\sigma(i)} \omega^{\tau i} / W_{o_\sigma(i)}$.

Coherent Estimate For $i \in \hat{I}$, estimate $\hat{X}_i = \texttt{median}\{\hat{X}_i^{(l)} : i \in \hat{I}\}$, taking real and imaginary parts separately.

As stated, the sFFT runs L location inner loops followed by another L estimation inner loops. In practice, it is not necessary to re-run the inner loops for the estimation steps if the alogirhtm keeps track of the σ_l and τ_l used in each location loop.

III. Array-based Compressed Sensing Receiver Architecture

Consider a typical digital phased array receiver with N_r elements operating over a tuning bandwidth of W_t with an instantaneous bandwidth of W_i. In each channel of the array, mixers downconvert a narrowband signal of interest centered at f_c to an intermediate frequency (IF) or to DC ("zero IF") where the signal is filtered to bandwidth W_i to reduce noise and avoid aliasing. Following another downconversion when necessary, the signal is sampled at the Nyquist rate of $2W_i$ (or W_i if IQ sampling is used). Array processing techniques are then applied to the samples collected from each channel to, e.g., form receive beams pointed in particular directions. While digital arrays allow beams to be formed in several directions simultaneously, received signals must lie within the W_i Hertz band set by the LO frequency.

ACRA makes a few minor changes to a typical digital receiver array in order to drastically expand the bandwidth via sFFT-inspired signal processing. Rather than tuning the receiver to f_c and filtering the signal to bandwidth W_i, ACRA sets the LO to the center of the tuning band and passes the entire tuning band with bandwidth W_t to the ADCs in each channel. The ADCs in each array channel are clocked at different rates, allowing each channel to digitize a different aliased version of the signal. These downsampled versions of the wideband signal play the role of the downsampled data streams in the sFFT.

A. Hardware Modifications

ACRA relies on aliasing of tuning bandwiths which are significantly wider than typical instantaneous bandwidths. This can be a challenge for many existing high speed ADCs (≥ 1 GSPS), which are not designed to alias several Nyquist zones having input bandwidths typically between f_s and $2f_s$. At the chip level, this limitation can be addressed by designing ADCs with input bandwidths matching W_t. At the component level, a wideband track-and-hold amplifier (THA) can be added directly before the ADC in each channel to increase the input bandwidth of the ADC. The THA effectively takes on the sampling role, while the ADC acts as a quantizer.

ACRA makes slight modifications to front-end hardware in typical digital phased arrays to accomodate the downsampling and aliasing necessary for the sFFT. Slight modifications to the sFFT are necessary to estimate AoA.

B. Algorithm Modifications

Note that the sFFT does not use the delay (given by τ) between the start of different downsampled data streams to determine the frequency support of the signal. This delay is only used in the estimation step to undo the different phase shifts occuring in each set of downsampled data. In other words, detection of frequency support uses a form of incoherent combining, while estimation uses coherent combining.

In a receiver array AoA information resides in the relative phase offsets of signals from different channels making it necessary to coherently combine signals from each antenna to estimate AoA. If the signals impinging on the array occupy a sparse set of frequencies, then the location step of the sFFT can be used to determine frequency support and the estimation step can be augmented with phase adjustments corresponding to different putative angles of arrival and antenna locations.

If the signals impinging on the array are not sufficiently frequency-sparse, but are sparse in frequency-angle space, incorporating AoA estimation into the voting step may be more appropriate. This can be accomplished by coherently combining estimates from each antenna. Thus $s_i = |\{l : i \in I_l\}|$ is replaced with:

$$s_{k,\theta,\phi} = \left| \sum_{l=1}^{L} \frac{Z_{h_{\sigma_l}(k)} e^{j \frac{2\pi}{N} k(\tau_l + \zeta_l(\theta,\phi))}}{W_{o_{\sigma_l}(k)}} 1_{|Z_{h_{\sigma_l}(k)}| \geq T_h} \right| \quad (1)$$

where $\zeta_l(\theta, \phi)$ is the time delay at antenna l due to its position in the array for a signal impinging on the array at angle (θ, ϕ) and 1_E is the indicator function for event E. If $s_{k,\theta,\phi} \geq T_d$, a detection is declared for a signal at frequency k and angle (θ, ϕ).

Using coherent combining in the voting step replaces the integer random variable s_i with a continuous random variable $s_{k,\theta,\phi}$ related to the strength of the signal. This can have a profound effect on the dynamic range of detectable signals. In the incoherent case (i.e. voting), the dynamic range is limited by the noise present in each channel. Under coherent

combining, the dynamic range is limited to $20 \log_{10} N_r$ dB unless an iterative version of the sFFT is used (e.g. [9]). Thus, signals which are sparse in frequency-angle space, but not sufficiently sparse in frequency alone, may require additional computation to maintain high dynamic range.

We make a few other modifications to the sFFT. Whereas the original algorithm uses randomly selected σ_l in $[N]$, ADC maximum sampling rates place a lower bound on σ_l. This has only minor effects on algorithm performance. Also, rather than finding the dk entries of maximum magnitude in Z, we add a threshold requiring that $|Z_i| \geq T_h$ (as seen in Eq. 1).

IV. Simulations

We next demonstrate frequency and AoA estimation using ACRA via simulation. While it is possible to combine ACRA's time domain undersampling with undersampling in the spatial domain via a sparse array (e.g. [10], [11]), we chose to use a uniform linear array (ULA) for simplicity. The interplay between sparse array considerations and time domain downsampling is an ongoing area of research.

We simulate reception of signals in the 32 GHz band between 18 and 50 GHz using ADCs operating between 1 and 2 GSPS. The simulated array spacing is 3 mm corresponding to $\lambda/2$ for 50 GHz. We use 8 unique sampling rates and 16 antenna elements. Each sampling rate is used twice with the assignments made by a random permutation. We used 64-QAM OFDM signals with 12 subcarriers spaced 240 kHz apart so that the signals of interest are only approximately sparse in frequency. The subcarrier frequencies do not align with the DFT bins used in the sFFT reconstruction. Signals were collected at relatively high SNR ($\sim$ 28 dB per channel), but noise folding effects were included.

Figure 1 shows the result of using ACRA to detect 5 OFDM signals of equal power centered at 18.63, 18.87, 21.58, 25.96, and 29.51 GHz with corresponding angles of arrival of -31.02, 24.31, 47.35, -8.60, and -6.95 degrees ($\sin(\theta) = -0.52$, 0.41, 0.74, -0.15, and -0.12, respectively). As shown in Fig. 1a, we used incoherent voting to determine frequency bands with significant energy. Once these bands are determined, the time domain signals from each antenna can be synthesized at the Nyquist rate. These synthesized Nyquist signals can then be used in conventional beamforming approaches. The beamscan estimate is shown in Fig. 1b with each column corresponding to a different frequency bin detected by the sFFT. In this case, ACRA detected 26 frequency bins clustered into 5 groups. The signals are detected at the correct frequencies and at the correct AoA. For comparison, the beanscan result for signals collected at the Nyquist rate are shown in Fig. 1c.

Next, we repeat the same experiment, but with the 5 signals at the same frequency with different angles of arrival. ACRA correctly selects four frequency bins surrounding the common carrier frequency. Figure 2 shows the estimated spatial spectra at these frequencies. The traces are nearly identical to those of the Nyquist rate beamscan (not shown).

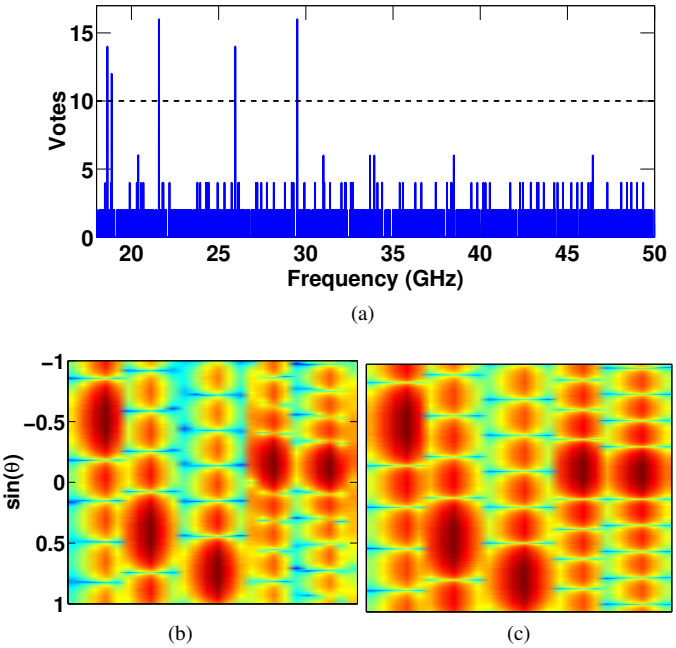

Fig. 1: Results of simulating ACRA reception of 5 OFDM signals at different frequencies and angles of arrival. (a) The sFFT voting step isolates frequencies agreed upon by at least 10 of 16 channels. Time domain signals are then synthesized at the Nyquist rate using the selected frequencies to build a basis. (b) The synthesized signals are combined using a beamscan approach at the 26 frequency bins selected in (a). (c) The beamscan result using Nyquist rate samples for comparison.

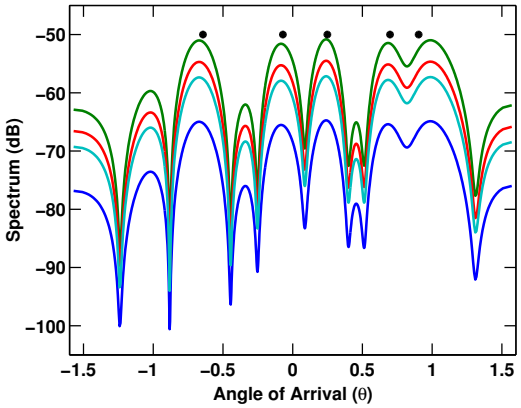

Fig. 2: ACRA beamscan spectrum when 5 OFDM signals lie in the same frequency at different angles of arrival. Solid lines represent spatial spectra for four neighboring frequency bins with detected energy. Black dots illustrate true angles of arrival (at an arbitrary power level).

V. Testbed

As described in Sec. III-A, some minor hardware modifications may be necessary to convert a typical tuned array to an ACRA array. We have constructed an 18–45 GHz testbed using

discrete commercial off-the-shelf (COTS) RF components to verify feasibility of the approach. The testbed comprises 8 channels capable of operating at 4 different sampling rates up to 2 GSPS. We are in the process of integrating an antenna array for over-the-air testing. The remainder of this section addresses some practical concerns regarding wideband millimeter wave components.

The key hardware requirement in ACRA is the need for ADC input bandwidth spanning several Nyquist zones. Most COTS ADCs are designed to be used with an anti-alias filter; thus, their internal track-and-hold circuits are not designed for bandwidths many times the maximum samping rate. Our testbed uses 2 GSPS ADCs (SP Devices, ADQ412-4G-cPCIe/PXIe) with datasheet input bandwidth of 2 GHz. We use THA evaluation boards (Hittite, EVAL01-HMC661LC4B) in front of the ADCs to increase the input bandwidth to 18 GHz.

IQ sampling is required to increase the input bandwidth beyond the 18 GHz provided by the THAs; however, frequency-dependent mismatches in the I and Q paths of the receivers can cause images to appear in the sampled signal. Marki MLIQ-1845L IQ mixers are used in the testbed to maximize the image rejection ratio (IRR) while allowing an input band of 18–45 GHz. Unfortunately, the mixers alone are not responsible for the system IRR. Mismatches in the filters, THAs, ADCs, and cables that follow the mixers can increase IRR. We use digital compensation to correct for IQ mismatch in the receive chains of each channel. An example for a single channel is shown in Fig. 3. Looking across all channels, we have obtained an average IRR of 40.6 dB.

Digital IQ compensation applies amplitude and phase adjustments to the Q channel which depend on the frequency of the input signal. Using ACRA, the frequency of a signal in a single channel is ambiguous by design, making it impossible to know which IQ compensation adjustments to apply. We make slight modifications to accomodate IQ compensation.

First, when detecting large magnitude signals in the Location Inner Loop of the sFFT, rather than use the magnitude of the coefficient in a given downsampled DFT bin, we use the sum of the absolute values of the frequency domain I and Q channel signals. This ensures that we will not miss a detection due to IQ mismatch.

Second, when unfolding each detected signal to its possible source frequencies bins $i \in I_l$ (Step 3 of the Location Inner Loop of the sFFT), we apply the IQ adjustments corresponding to each possible source frequency and check to see if the signal magnitude still exceeds the threshold T_h.

Figure 4 shows successful detection of two tones on our ACRA testbed. The tones were generated at 24.7 and 38.2 GHz and applied to 4 channels of the testbed. The signals were mixed to baseband with a 34 GHz LO in each channel and subsequently sampled at 1.3913, 1.5238, 1.6842, and 1.8824 GSPS. We applied sFFT processing with digital IQ compensation to detect the two signals at the appropriate frequencies.

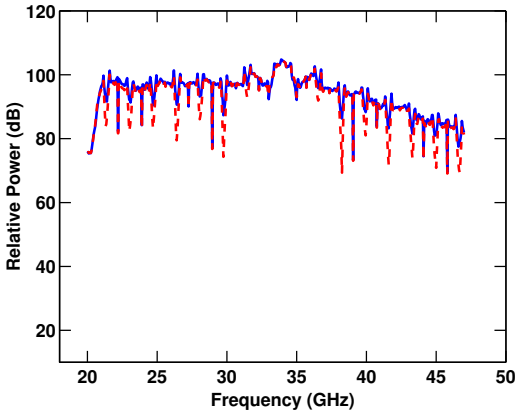

(a)

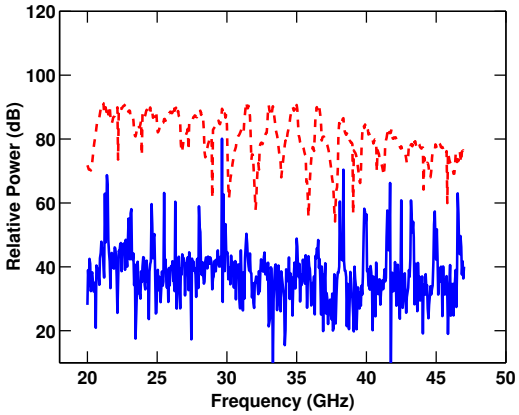

(b)

Fig. 3: Digital IQ compensation in a single ACRA channel. Red, dashed lines show power before calibration, while blue, solid lines show power after calibration for tones (a) and images (b).

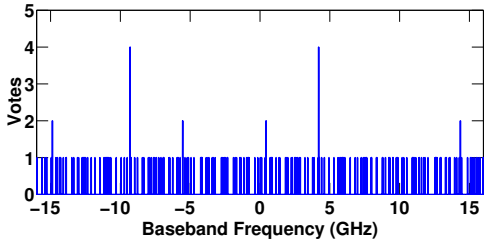

Fig. 4: Successful detection of tones at -9.3 and 4.2 GHz complex baseband on ACRA testbed using 4 channels at 4 different sampling rates. Images are suppressed via digital IQ compensation.

VI. Summary

The proposed Array-based Compressed sensing Receiver Architecture allows wideband receiver arrays to operate with significantly higher instantaneous bandwidths. The approach requires only minor modifications to typical receiver array

hardware and leverages sFFT signal processing to detect, localize, and estimate signals. We have presented some simulation results as well as initial experiments from our 18–45 GHz testbed demonstrating the feasibility of the approach.

We are currently exploring many intriguing possibilities with ACRA. These include the use of sparse arrays, adaptive array processing, and signal estimation in dense environments.

REFERENCES

[1] E. J. Candès, J. K. Romberg, and T. Tao, "Robust uncertainty principles: exact signal reconstruction from highly incomplete frequency information," *IEEE Transactions on Information Theory*, vol. 52, no. 2, pp. 489–509, 2006. [Online]. Available: http://dx.doi.org/10.1109/TIT.2005.862083

[2] D. L. Donoho, "Compressed sensing," *IEEE Transactions on Information Theory*, vol. 52, no. 4, pp. 1289–1306, 2006. [Online]. Available: http://dx.doi.org/10.1109/TIT.2006.871582

[3] J. Laska, S. Kirolos, Y. Massoud, R. Baraniuk, A. Gilbert, M. Iwen, and M. Strauss, "Random sampling for analog-to-information conversion of wideband signals," in *IEEE Dallas Circuits and Systems Workshop (DCAS)*, 2006.

[4] M. Mishali and Y. C. Eldar, "From theory to practice: Sub-Nyquist sampling of sparse wideband analog signals," *J. Sel. Topics Signal Processing*, vol. 4, no. 2, pp. 375–391, 2010. [Online]. Available: http://dx.doi.org/10.1109/JSTSP.2010.2042414

[5] T. Murray, P. Pouliquen, A. Andreou, and K. Lauritzen, "Design of a CMOS A2I data converter: Theory, architecture and implementation," in *Information Sciences and Systems (CISS), 2011 45th Annual Conference on*, March 2011, pp. 1–6.

[6] M. Trakimas, T. Hancock, and S. R. Sonkusale, "A compressed sensing analog-to-information converter with edge-triggered SAR ADC core," in *2012 IEEE International Symposium on Circuits and Systems, ISCAS 2012, Seoul, Korea (South), May 20-23, 2012*, 2012, pp. 3162–3165. [Online]. Available: http://dx.doi.org/10.1109/ISCAS.2012.6271993

[7] A. Gilbert, P. Indyk, M. Iwen, and L. Schmidt, "Recent developments in the sparse fourier transform: A compressed fourier transform for big data," *Signal Processing Magazine, IEEE*, vol. 31, no. 5, pp. 91–100, Sept 2014.

[8] H. Hassanieh, P. Indyk, D. Katabi, and E. Price, "Simple and practical algorithm for sparse fourier transform," in *Proceedings of the Twenty-third Annual ACM-SIAM Symposium on Discrete Algorithms*, ser. SODA '12. SIAM, 2012, pp. 1183–1194. [Online]. Available: http://dl.acm.org/citation.cfm?id=2095116.2095209

[9] H. Hassanieh, L. Shi, O. Abari, E. Hamed, and D. Katabi, "Bigband: Ghz-wide sensing and decoding on commodity radios," MIT CSAIL, Cambridge, MA, Tech. Rep. MIT-CSAIL-TR-2013-009, May 2013. [Online]. Available: http://hdl.handle.net/1721.1/79058

[10] D. Romero, D. Arianandа, Z. Tian, and G. Leus, "Compressive covariance sensing: Structure-based compressive sensing beyond sparsity," *Signal Processing Magazine, IEEE*, vol. 33, no. 1, pp. 78–93, Jan 2016.

[11] J. Krieger, Y. Kochman, and G. Wornell, "Design and analysis of multi-coset arrays," in *Acoustics, Speech and Signal Processing (ICASSP), 2013 IEEE International Conference on*, May 2013, pp. 3781–3785.